Nanoscale Res Lett (2009) 4:113–121
DOI 10.1007/s11671-008-9210-9

NANO EXPRESS

Folate Functionalized Boron Nitride Nanotubes and their Selective Uptake by Glioblastoma Multiforme Cells: Implications for their Use as Boron Carriers in Clinical Boron Neutron Capture Therapy

Gianni Ciofani · Vittoria Raffa · Arianna Menciassi · Alfred Cuschieri

Received: 17 October 2008 / Accepted: 11 November 2008 / Published online: 25 November 2008

Abstract Boron neutron capture therapy (BNCT) is increasingly being used in the treatment of several aggressive cancers, including cerebral glioblastoma multiforme. The main requirement for this therapy is selective targeting of tumor cells by sufficient quantities of ^{10}B atoms required for their capture/irradiation with low-energy thermal neutrons. The low content of boron targeting species in glioblastoma multiforme accounts for the difficulty in selective targeting of this very malignant cerebral tumor by this radiation modality. In the present study, we have used for the first time boron nitride nanotubes as carriers of boron atoms to overcome this problem and enhance the selective targeting and ablative efficacy of BNCT for these tumors. Following their dispersion in aqueous solution by noncovalent coating with biocompatible poly-L-lysine solutions, boron nitride nanotubes were functionalized with a fluorescent probe (quantum dots) to enable their tracking and with folic acid as selective tumor targeting ligand. Initial in vitro studies have confirmed substantive and selective uptake of these nanovectors by glioblastoma multiforme cells, an observation which confirms their potential clinical application for BNCT therapy for these malignant cerebral tumors.

G. Ciofani · V. Raffa · A. Menciassi · A. Cuschieri
Scuola Superiore Sant'Anna, Piazza Martiri della Libertà, 33, 56127 Pisa, Italy

G. Ciofani (✉)
Scuola Superiore Sant'Anna, CRIM Lab - Center for Applied Research in Micro and Nano Engineering, Viale Rinaldo Piaggio, 34, 56025 Pontedera (Pisa), Italy
e-mail: g.ciofani@sssup.it

A. Menciassi
Italian Institute of Technology (IIT), Via Morego, 30, 16163 Genoa, Italy

Keywords Boron nitride nanotubes · Folate · Glioblastoma multiforme · Boron neutron capture therapy

Introduction

High-grade glioblastoma multiforme is uniformly fatal and largely unresponsive to all available treatments. Patients with these tumors usually survive for <1 year from the time of first diagnosis. Conventional surgical excision, generally limited to the main tumor mass, does not remove the microscopic foci of neoplastic cells that invade the surrounding normal brain substance beyond the main tumor mass, and are responsible for the inevitable tumor recurrence [1]. Conventional radiotherapy cannot ablate completely these tumors [2], since this would require unacceptably high radiation doses that result in severe brain damage [3]. Boron neutron capture therapy (BNCT) is a binary modality therapy that has the potential for effective treatment of many forms of cancers, including cerebral glioblastoma multiforme brain and melanomas [4–6]. BNCT is based on the neutron capture reaction, $^{10}B(n, \alpha)^{7}Li$, where a ^{10}B atom captures a low-energy thermal neutron and spontaneously decays to produce the linear recoiling particles ^{4}He (α particle) and ^{7}Li. In tissues, these particles have short penetration ranges, approximately the width of a single cell (5 μm for ^{7}Li and 9 μm for ^{4}He). As the average linear energy transfer is high (^{7}Li, 162 keV/μm; ^{4}He, 196 keV/μm), this results in densely ionizing radiation restricted to the track of each particle [7, 8]. Thus, the essential requirement for effective BNCT is selective targeting of tumor cells with sufficient quantities of ^{10}B atoms (15–30 μg/g or more) and their irradiation with low-energy thermal neutrons. In theory, BNCT is potentially capable of killing individual cancer cells while sparing the healthy normal parenchyma. Consequently,

knowledge of the micro distribution of ^{10}B from boronated drugs in cells of cancerous and normal tissues is of critical importance [9]. The ideal drug would provide boron selectively to tumor cells and would be nontoxic to normal cells. Experimentally, cell culture tumor models provide a useful approach for the investigation and understanding the mechanisms of boron delivery by BNCT agents to cancer and normal cells [10, 11]. The problem, however, is that there is currently no truly satisfactory ^{10}B target agent for any human tumor type [12] although several boron agents have been proposed and synthesized, but many of these have either one or more disqualifying features [13]. The ability of BNCT to fulfill its clinical therapeutic potential thus clearly rests on the discovery and availability of effective and safe boron transport agents.

In the present preliminary study, we have investigated the use of boron nitride nanotubes (BNNTs) as boron atom carriers. BNNTs are structural analog of carbon nanotubes (CNTs) with alternating B and N atoms which entirely substitute for C atoms in a graphitic-like sheet with almost no change in atomic spacing. Thus, BNNTs are composed of a substantial number of boron atoms (about 50%) equivalents to hundreds to thousands per each nanotube. Hence our hypothesis underlying the present investigation is that BNNTs may serve as effective boron targets for BNCT. BNNTs have generated considerable interest within the scientific community by virtue of their unique properties. As with CNTs, they have various potentially useful structural and electronic applications [14, 15] and share good flexibility with CNTs with a Young modulus of 1.22 ± 0.24 TPa [16, 17] but have superior chemical and thermal stability. Together with their high resistance to oxidation and stability [18], these properties mark BNNTs as attractive potential candidates for a wide range of applications. Nevertheless, in sharp contrast to the many proposed biomedical applications of CNTs in recent years, e.g., biosensors, DNA chip, nanovectors for drug, protein and gene delivery [19], etc., the use of BNNTs in this field has been largely unexplored [20]. Cytocompatibility studies and the interaction between BNNTs and living cells have only been reported recently [21, 22] by our group and other biomedical applications concerning their magnetic properties are actively under investigation in our laboratory.

In the present study, we realized stable dispersions of BNNTs employing a positively charged protein (ploy-L-lysine, PLL) as dispersion agent. Poly-L-lysine coated BNNTs were then conjugated with fluorescent molecules (quantum dots) to enable their tracking in living cells. Folic acid was used as a targeting ligand to functionalize BNNTs against tumor cells, because of the ease of the reaction procedure and the small size of the folate molecule, enabling a stable binding with the nanotube coating, thus permitting folate receptor-mediated endocytosis of PLL-BNNTs. To date, folate has been used as a targeting ligand for both tumor imaging and cancer chemotherapy [23–26].

The functionalized BNNTs were characterized by imaging, Z-potential, size distribution, and UV–Vis spectra. In vitro uptake tests were carried out on human glioblastoma multiforme cells and on healthy human primary fibroblasts as controls.

Materials and Methods

BNNT Dispersion and Functionalization

Boron nitride nanotubes provided by the Australian National University, Canberra, Australia, were produced by using a ball-milling and annealing method [27, 28]. These samples contain the ^{11}B isotope. As the chemical and biological interactions are independent on the isotope type, we can assume the same results can be achieved with ^{10}B containing (used in clinical BNCT). Details of sample purity and composition (provided by the supplier) are as follows: yield >80%, boron nitride >97 wt%, metal catalysts (Fe and Cr) derived from the milling process $\sim$1.5 wt% and absorbed O_2 $\sim$1.5 wt%.

The polymer used for the aqueous suspension and dispersion of BNNTs was PLL obtained from Fluka (81339), MW 70,000–150,000. All experiments were carried out in phosphate buffered solution (PBS) as described previously [21, 22]. Briefly, samples of BNNT powder in a 0.1% PLL solution were ultrasonicated for 12 h with a Branson sonicator 2510 (Bransonic). The output power of sonicator was fixed at 20 W for all experiments. Next, the sample was centrifuged at $1{,}100\times g$ for 10 min to remove nondispersed residuals and impurities. Excess PLL was removed by ultracentrifugation three times at $30{,}000\times g$ for 30 min at 4 °C (Allegra 64R, Beckman) and stable PLL-BNNT dispersion was obtained as a result of the noncovalent coating of the nanotube walls with PLL.

Folate conjugation was achieved by linking the amino-groups of PLL with the γ carboxylic-groups of the folate molecules, which are not involved in the folate receptor interaction [29]. Folic acid (F7876 from Sigma), 3.5, and 5 mM 1-ethyl-3-(3-dimethylamino-propyl) carbodiimide (EDC, 03450 from Fluka) were added to a dispersion of 50 μg/mL of PLL-BNNT [30]. After reaction, the dispersion was ultracentrifuged (three times at $30{,}000\times g$ for 30 min at 4 °C) to remove unbound folic acid and EDC resulting in stable dispersions of folate conjugated PLL-BNNT (F-PLL-BNNT).

Spectrophotometric analysis was carried out with a LIBRA S12 Spectrophotometer UV/Vis/NIR (Biochrom) to characterize the dispersions and to quantify BNNT concentrations [21].

Both the dispersed PLL-BNNTs and F-PLL-BNNTs were covalently labeled with carboxyl derivatised quantum dots for cellular tracking studies. Carboxyl quantum dots were supplied by Invitrogen (Qdot® 605 ITK™). The conjugation reaction between the amino-groups of PLL and carboxylic-groups of quantum dots was carried out as specified by the supplier. Briefly, 4 mL of PLL-BNNT (50 μg/mL) were mixed with 4 μL of Qdots (8 μM) and 60 μL of EDC, 10 mg/mL, as activator. The solution was gently stirred for 90 min at room temperature for optimal conjugation and finally centrifuged (1,000×g, 10 min) to remove large aggregates. Finally, ultracentrifugation (twice at 30,000×g for 30 min at 4 °C) was performed to remove unbound quantum dots and obtain the labeled BNNT dispersions. Even if quenching of quantum dot fluorescence can occur because of some electron transfer between BNNTs and fluorescence dyes [31], the final product results perfectly suitable for biological tracking [22].

Sample size distribution was analysed with an N4plus submicron particle size analyser (Beckman Coulter); Z-potential measurement was performed with a Nano Z-Sizer (Malvern Instrument). Each acquisition was performed three times on aqueous nanotube suspensions of concentration 1 μg/mL.

Samples were imaged by Focused Ion Beam (FIB) microscopy which allows high contrast imaging [32]. For this purpose, a small drop (10 μL) of PLL-BNNT dispersion (5 μg/mL) was placed onto a plasma-cleaned silicon wafer and air dried. The FIB system used was a FEI 200 (Focused Ion Beam localized milling and deposition) delivering a 30 keV beam of gallium ions (Ga^+). Figure 1a shows well dispersed F-PLL-BNNTs after the completion of the preparation procedure.

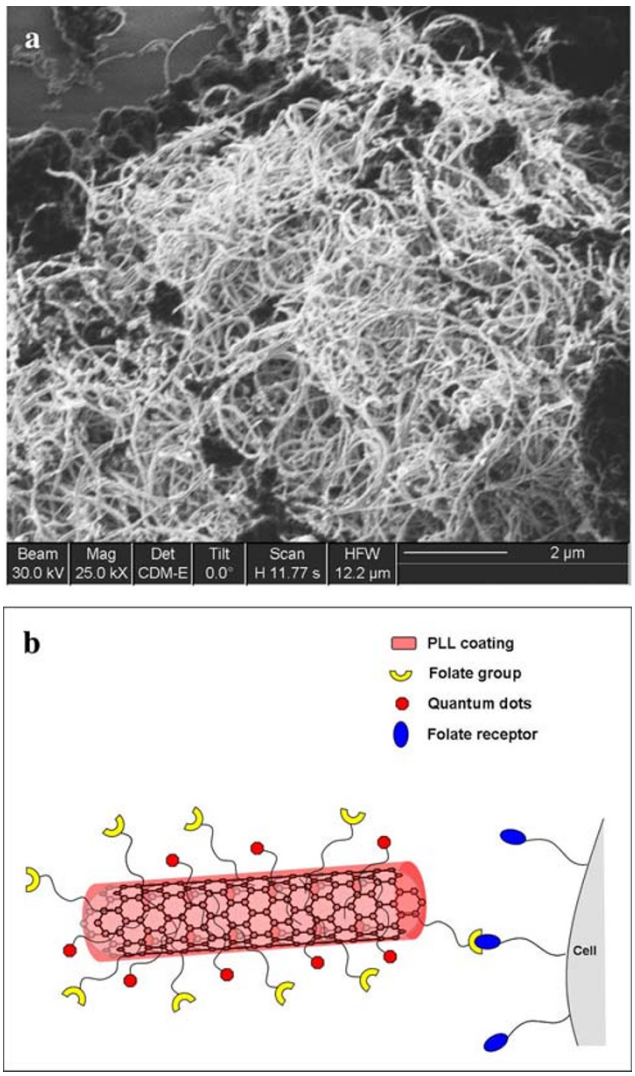

Fig. 1 FIB image of well dispersed F-PLL-BNNTs (**a**); diagram of the proposed nanovector (**b**)

Cell Cultures and Viability Assay

Human glioblastoma multiforme T98G cells (ATCC CRL-1690) were cultured in Dulbecco's modified Eagle's medium with 10% fetal bovine serum, 100 IU/mL penicillin, 100 μg/mL streptomycin, and 2 mM L-glutamine. Primary human gingival fibroblasts (gift from Dr. Stefania Moscato, University of Pisa) were cultured in the same medium with the addition of 10 ng/mL of epidermal growth factor (EGF). Cells were maintained at 37 °C in a saturated humidity atmosphere containing 95% air/5% CO_2 and were seeded in a 24-well plate (30,000 cells/well).

For viability testing, MTT (3-(4,5-dimethylthiazole-2-yl)-2,5-diphenyl tetrazolium bromide, M-2128 from Sigma) cell proliferation assays were carried out after 24 h of incubation with PLL-BNNT and F-PLL-BNNT modified media, which contained 10% BNNT dispersion, corresponding to a final concentration of 10 μg/mL of BNNT. After trypsinization and counting with a Burker chamber, each cell culture was subdivided and seeded in six 96-well plate chambers. Once the adhesion was verified (after about 6 h from the seeding) cells were incubated with MTT 0.5 mg/mL for 2 h. After cell treatment with 100 μL of DMSO (dimethyl sulfoxide, D8418 from Sigma) absorbance at 550 nm was measured with a VERSAMax microplate reader (Molecular Devices). A reference control test (k-) was carried out.

Cellular Uptake Studies

After adhesion (at 6 h), the cells were treated for 90 min with the Qdots labeled PLL-BNNT and F-PLL-BNNT modified culture medium (final concentration 10 μg/mL of BNNTs). In a control experiment, folic acid was added to the cell culture medium to compete with the F-PLL-BNNTs. For this competitive inhibition experiment, folic

acid was first added to the medium at a concentration of 3.5 mM and cells were incubated for 30 min. Subsequently, F-PLL-BNNTs were added and the cells were incubated for a further 90 min.

Lysosome tracking assays were carried out on glioblastoma cells with LysoTracker dye (L12491 from Invitrogen). This is a fluorescent acidotropic probe for labeling acidic organelles in live cells. The probe fluoresces when it accumulates in cellular compartments with low pH. For these studies, cells were incubated 2 h in a growth medium containing LysoTracker in a dilution of 1:2,500 after 90 min exposure to F-PLL-BNNT in the medium.

Cell imaging was carried out with a Nikon TE2000U fluorescent microscope equipped with a Nikon DS-5MC USB2 cooled CCD camera. The cellular uptake of labeled

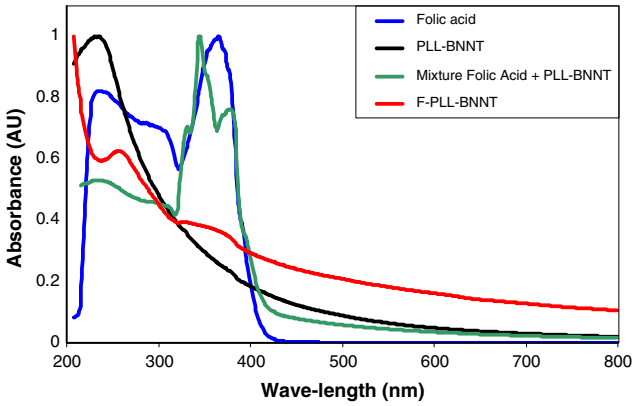

Fig. 2 UV–Vis spectra of folic acid, PLL-BNNTs, a mixture of folic acid and PLL-BNNTs, and F-PLL-BNNTs

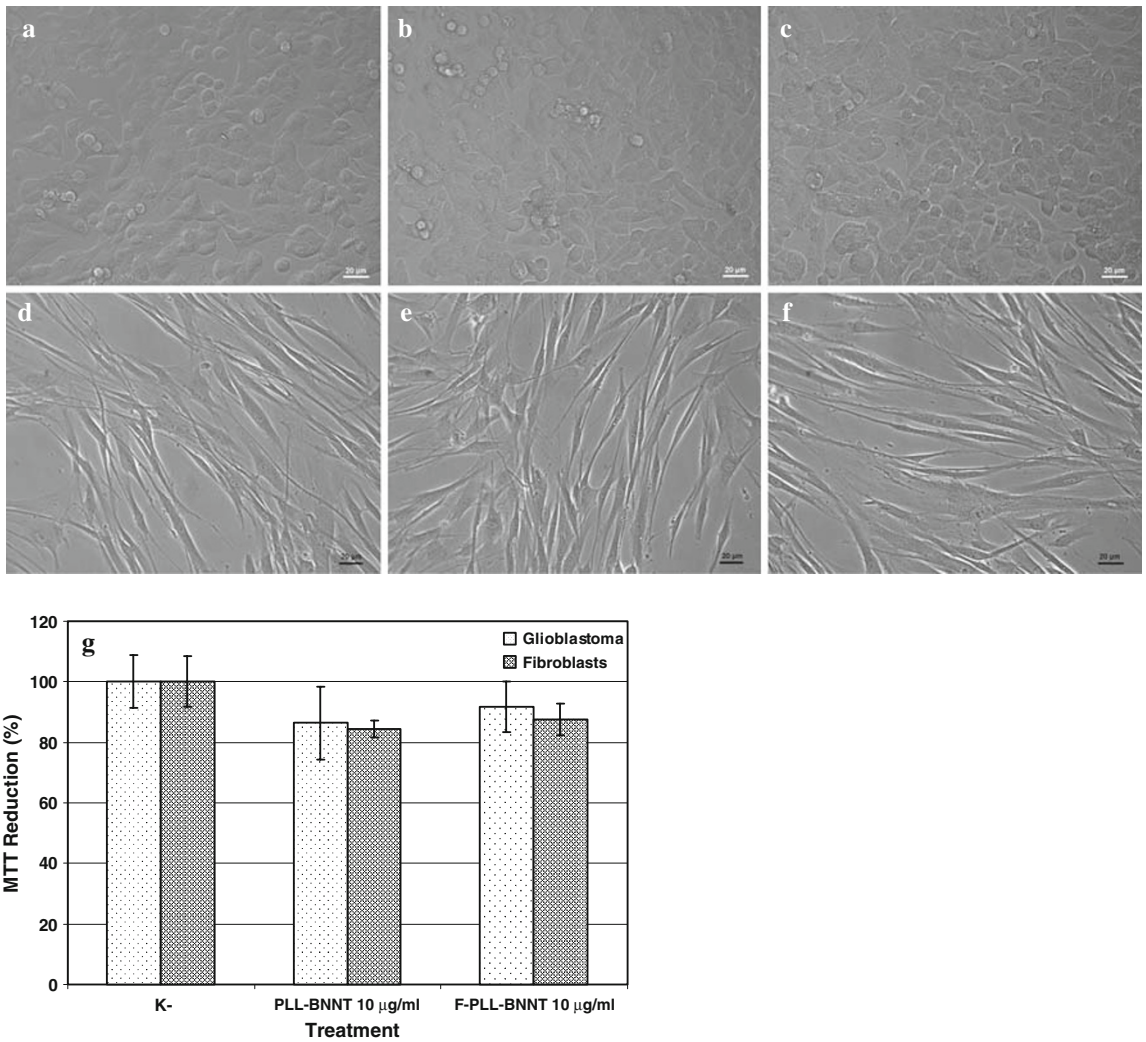

Fig. 3 Morphology, after 24 h of treatment, of glioblastoma control culture (**a**); glioblastoma incubated with 10 μg/mL of PLL-BNNTs (**b**); glioblastoma incubated with 10 μg/mL of F-PLL-BNNTs (**c**); fibroblast control culture (**d**); fibroblasts incubated with 10 μg/mL of PLL-BNNTs (**e**); fibroblasts incubated with 10 μg/mL of F-PLL-BNNTs (**f**); and MTT results for all the tests (**g**)

BNNT was determined by the fluorescence intensity obtained from the acquired images, and this provided a measure of the nanotubes concentration inside the cells. Before imaging, BNNT-incubated cells were washed three times with PBS buffer after each experiment.

Each image was analysed with a dedicated MatLab program for extrapolation of the fluorescence intensity. In particular, every color channel component (R, G, B) of the images was analysed. The average intensity of the R channel was then calculated and normalized to the maximum mean intensity obtained during all the experiments.

Statistical Analysis

The results were analysed by analysis of variance (ANOVA) followed by Student's t test to establish statistical significance which was set at 5%. MTT tests were performed in sixplicate; while for fluorescence analysis six images were acquired for each experiment. In all cases, three independent experiments were carried out. Results are presented as mean value ± SEM.

Results and Discussion

BNNT Characterization

Figure 1a shows a FIB image of dispersed BNNTs. Since the surface of many tumor cells over-expresses the folate receptor, while the surface of the normal cells exhibits only minimal expression, the folic acid functionalized PLL-BNNTs can be internalized by the tumor cells though the specific binding of the folic acid molecules present on the wall of the functionalized BNNTs with the surface folate

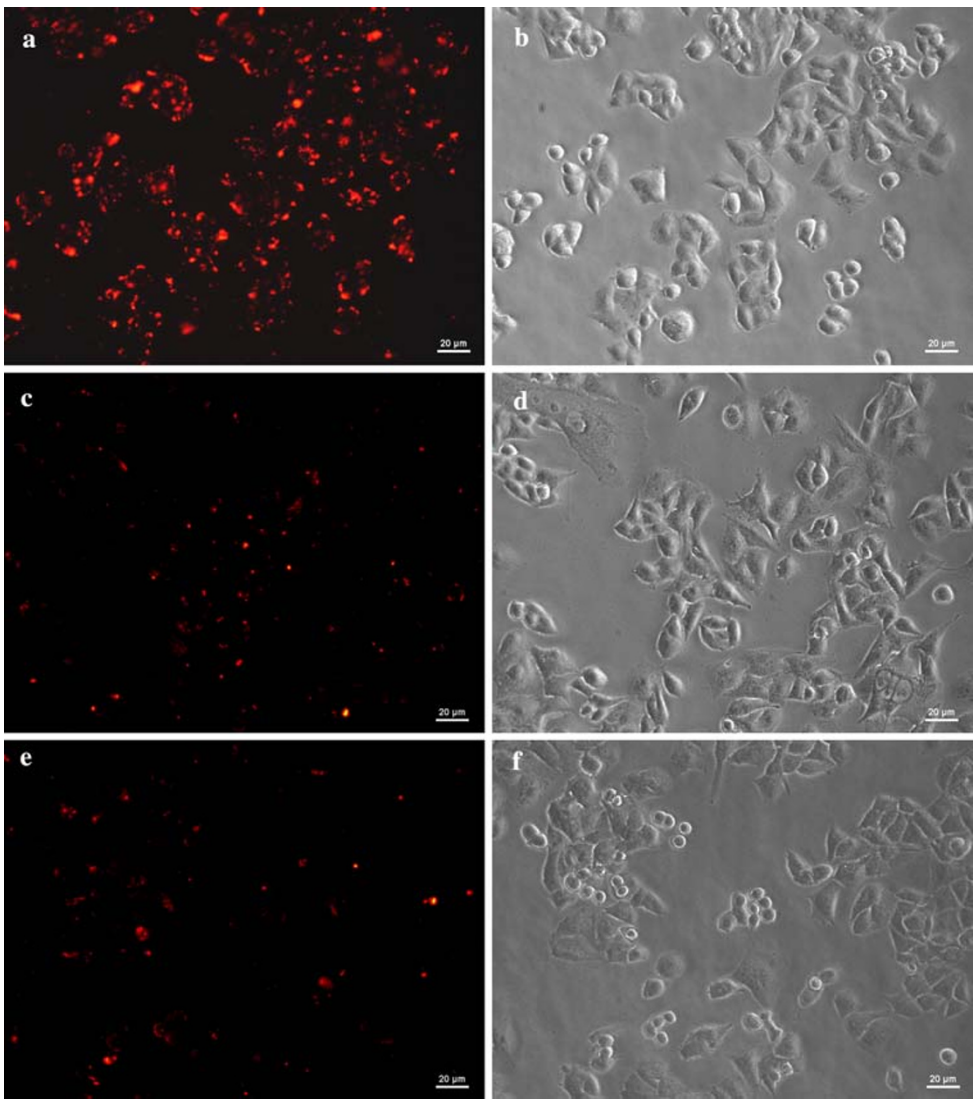

Fig. 4 Fluorescence image of glioblastoma cells incubated with 10 μg/mL of Qdot conjugated F-PLL-BNNTs (**a**); PLL-BNNTs (**c**); F-PLL-BNNTs with preincubation of 3.5 mM free folate (**e**). **b**, **d**, and **f** are the corresponding bright field images

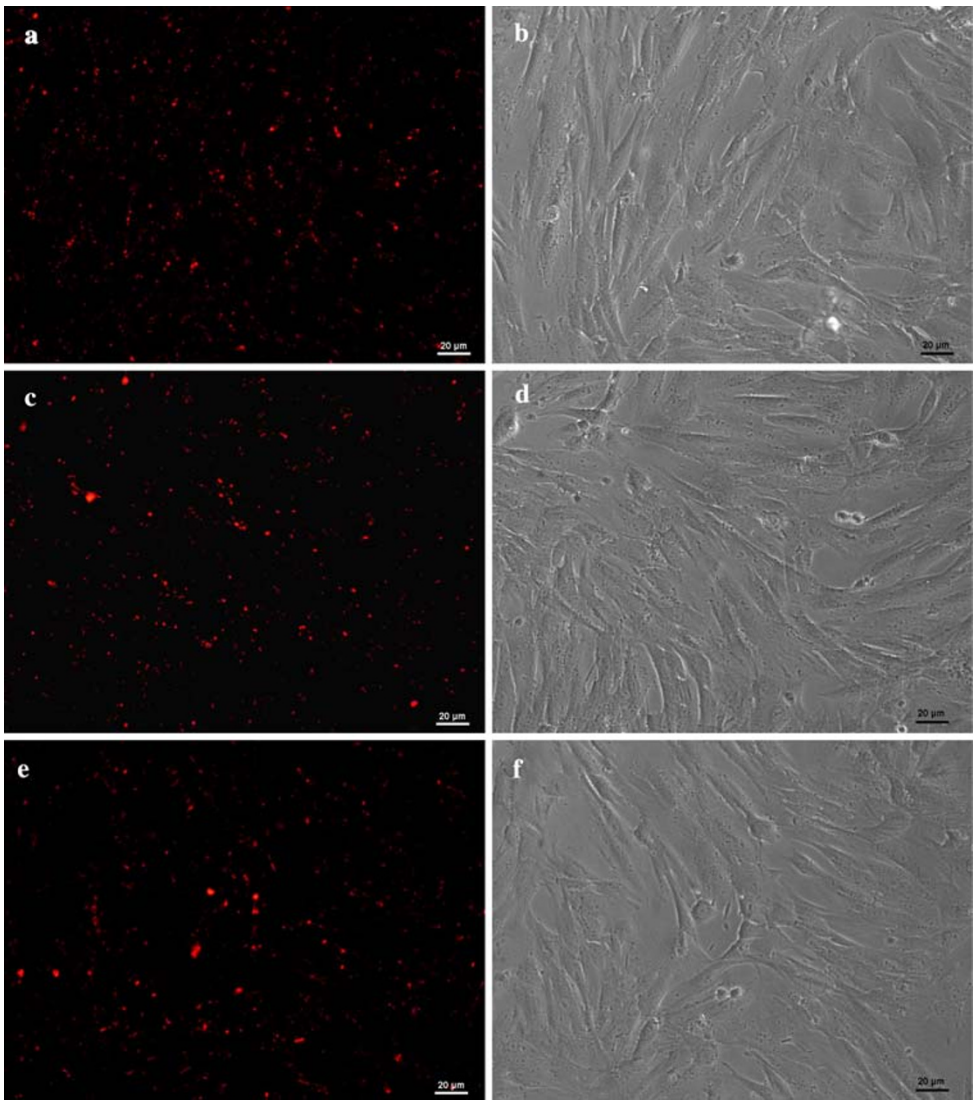

Fig. 5 Fluorescence image of fibroblast cells incubated with 10 μg/mL of Qdot conjugated F-PLL-BNNTs (**a**); PLL-BNNTs (**c**); F-PLL-BNNTs with preincubation of 3.5 mM free folate (**e**). **b**, **d**, and **f** are the corresponding bright field images

receptors of the tumor cells. The basic idea of this concept is illustrated in Fig. 1b. A similar approach has been reported to enhance cellular uptake of CNTs [30].

Spectrophotometric analysis was carried out after each experiment to verify the binding of folic acid with the PLL-BNNTs (Fig. 2). Folic acid exhibits a strong absorbance at 240 nm, a shoulder peak at about 290 nm, and a further strong peak at 370 nm; whereas PLL-BNNTs have just one absorbance peak at around 235 nm. F-PLL-BNNT dispersions exhibit a peak at 260 nm and a weak shoulder at about 360 nm. These absorbance shifts resulted from the interaction of PLL-BNNTs and folic acid, confirming successful chemical conjugation. The spectrum of a simple mixture of PLL-BNNT dispersion with the solution of folic acid, without reaction induced by EDC, was obtained as a control which showed that both the peaks and the shoulder peak of the folic acid were detectable at the same wavelength as that of the "free" folate.

Z-potential analysis confirmed the conjugation of folic acid with the PLL-BNNTs by revealing a strong positive Z-potential (43.4 ± 3.26 mV) for PLL-BNNTs; while a shift to -32.0 ± 2.51 mV was found for the F-PLL-BNNTs, thus indicating "masking" of the positive charges of PLL by the folate molecules.

The size distribution studies yielded an average value of 242 ± 92 nm for PLL-BNNTs and 479 ± 223 nm for the F-PLL-BNNTs.

In Vitro Experiments

Previously reported experiments, carried out on human neuroblastoma cells, have confirmed that these cells maintain good viability after 24 h of treatment with 5.0 μg/mL of polyethyleneimine coated BNNTs [22]. The present cultures confirmed the complete cytocompatibility of PLL-BNNTs with both glioblastoma and primary fibroblast

cells. No differences in cell morphology were observed between control (k-), PLL-BNNT and F-PLL-BNNT treatment culture. Figure 3a–c shows images of the three tests carried out on glioblastoma cells, whereas Fig. 3d–f provides images of the same tests on healthy fibroblast cells. Cell viability assessed with Trypan blue assay was >95% in each case. MTT assay, (Fig. 3g), provided clear evidence for excellent metabolic activity after 24 h of treatment. With both PLL-BNNT and F-PLL-BNNT treatments, metabolic activity exceeded 80% of the control for both the cell populations, with no significant difference between the experiments ($n = 6$; $p > 0.1$).

The binding of the receptors and their ligands has the characteristics of specificity, selectivity, strong affinity, and obvious biological effect. Thus in the present study, we have demonstrated that PLL-coated BNNTs functionalized with the folate ligand enable targeted uptake of the nanotubes by tumor cells by receptor-mediated endocytosis.

Even if the cells of glioblastoma multiforme do not have the high level expression of folate receptors encountered in other cancers [33], their increased expression relative to normal brain cells is well documented [34] and there has been several reports in the literature on targeted drug delivery for this tumor based on folate ligands [34, 35]. The folate ligand used in the present study to functionalize BNNTs against tumor cells, is particularly attractive because of the relative ease of the reaction procedure and the small size of the folate molecule enabling a more stable binding to the nanotube noncovalent PLL coating.

Qdots labeling of PLL-BNNTs allowed the direct visualization of the uptake by glioblastoma and healthy (control) fibroblast cells. The fluorescence image of glioblastoma cells after 90 min incubation in the presence of F-PLL-BNNTs is shown by Fig. 4a, in which intensive fluorescence was clearly observed, indicating significant cellular uptake of nanotubes; Fig. 4b shows the corresponding bright field image.

In sharp contrast, fluorescence of glioblastoma cells was considerably weaker when the cells were incubated for 90 min in the presence of not folate-functionalized PLL-BNNTs (Fig. 4c; with Fig. 4d corresponding bright field image). Figure 4e demonstrates that the folate-mediated cellular uptake of F-PLL-BNNTs could be blocked by competitive inhibition if a large amount of free folate (3.5 mM) was added into the culture medium for 30 min before the addition of F-PLL-BNNTs (Fig. 4f is the corresponding bright field image).

The same experiments were carried out on normal human gingival fibroblasts which acted as controls. In these experiments, similar but much weaker fluorescence intensity was detected in cultures treated with 10 μg/mL of F-PLL-BNNTs (Fig. 5a; bright field in Fig. 5b), with 10 μg/mL of nonfolate-functionalized PLL-BNNTs (Fig. 5c; bright field in Fig. 5d), and finally treated with F-PLL-BNNTs preceded by a preincubation of 3.5 mM free folate (Fig. 5e; bright field in Fig. 5f).

In summary, these results indicate that after 90 min of incubation with labeled PLL-BNNTs, the presence of the folate molecule on the BNNT coating strongly enhances the uptake by glioblastoma cells, but no appreciable improvement in uptake of the nanotubes is observed with normal cultured fibroblasts). Quantitative analysis of the fluorescence intensity, reported in Fig. 6a, confirms these data. The uptake of F-PLL-BNNTs by glioblastoma multiforme cells, in folate depleted medium, is statistically different ($p < 0.001$) and results in a 2-fold improvement with respect to all the other treatments, which show no statistically significant differences ($p > 0.05$).

Receptor-mediated endocytosis of F-PLL-BNNTs by glioblastoma multiforme cells is confirmed by Fig. 6b. This microphotograph consists of a high-magnification image of a glioblastoma cell following uptake of Qdot conjugated F-PLL-BNNTs and lysosomal tracking. Yellow

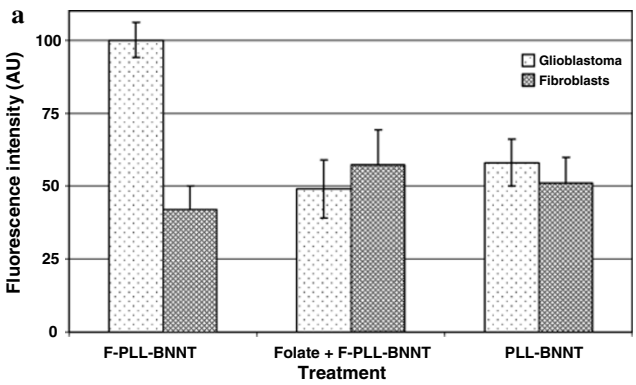

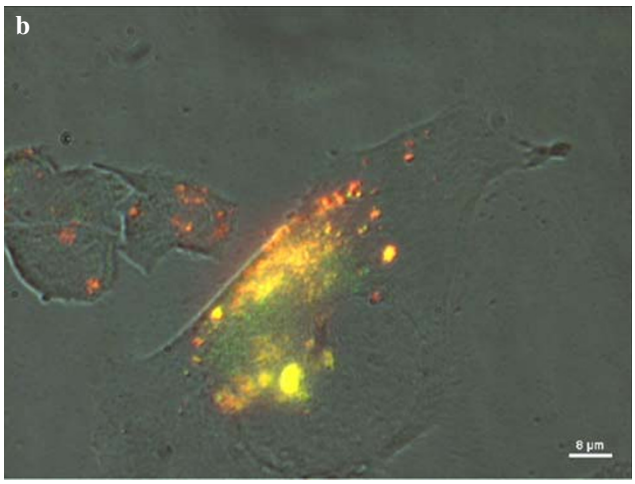

Fig. 6 Quantitative analysis of the fluorescence of glioblastoma and fibroblast cells following the three different treatments (**a**); high-magnification image of a glioblastoma multiforme cell following uptake of Qdot conjugated F-PLL-BNNTs and lysosomal tracking (**b**). Yellow fluorescence arises from merging of Qdot (*red*) and LysoTracker probe (*green*)

fluorescence arises from merging of Qdot (red) and LysoTracker probe (green) and demonstrates therefore a strong accumulation of the nanovectors in the acidic compartments (lysosomes) of the cells.

Conclusions

The results of recent and ongoing clinical trials which confirm the safety of BNCT for the treatment of cerebral GBM highlight the immediate need for truly effective boron target agents [36, 37]. In the present s study, we have investigated the use of BNNTs as boron atom carriers. After their dispersion in biocompatible PLL solutions, BNNTs were functionalized with a fluorescent probe and with folic acid for tumor targeting.

The results obtained indicate that folate-functionalized BNNTs have the potential to act as a boron delivery agents to malignant glioblastoma cells as these preliminary in vitro studies have confirmed a strong and selective uptake of these nanotubes vectors by glioblastoma multiforme cells but not by normal human fibroblasts. Obviously extensive in vivo and preclinical tests are needed to explore the use of functionalized BNNTS as boron target agents for clinical BNCT [38].

Acknowledgments The work described in this paper was supported in part by the Italian Institute of Technology (IIT) Network and the NINIVE (Non Invasive Nanotransducer for In Vivo gene therapy, STRP 033378) project, co-financed by the 6FP of the European Commission. The authors gratefully thank Mr. Carlo Filippeschi for allowing access to and use of the FIB microscope; Dr. Stefania Moscato (University of Pisa) for supplying the human primary fibroblasts and, finally, Prof. Shinji Takeoka and Mr. Yosuke Obata (Waseda University, Tokyo) for the size distribution and Z-potential analyses.

References

1. P.C. Burger, P.J. Dubois, S.C. Schold Jr., K.R. Smith Jr., G.L. Odom, D.C. Crafts, F. Giangaspero, Computerized tomographic and pathologic studies of the untreated, quiescent, and recurrent glioblastoma multiforme. J. Neurosurg. **58**, 159–169 (1983)
2. A.C. Halperin, P.C. Bruger, D.E. Bullard, The fallacy of the localized supratentorial malignant glioma. Int. J. Radiat. Oncol. Biol. Phys. **15**, 505–509 (1988). doi:10.1016/S0360-3016(98)90036-0
3. F.J. Sullivan, L.L. Hersher, J.A. Cook, J. Smith, S.M. Steinberg, A.H. Epstein et al., National Cancer Institute (Phase II) study of high-grade glioma treated with accelerated hyperfractionated radiation and iododeoxyuridine: Results in anaplastic astrocytoma. Int. J. Radiat. Oncol. Biol. Phys. **30**, 583–590 (1994)
4. R.F. Barth, A.H. Soloway, R.G. Fairchild, Boron neutron capture therapy for cancer. Sci. Am. **263**, 100–106 (1990)
5. J.A. Coderre, G.M. Morris, The radiation biology of boron neutron capture therapy. Radiat. Res. **151**, 1–18 (1999). doi:10.2307/3579742
6. W.H. Sweet, The use of nuclear disintegration in the diagnosis and treatment of brain tumor. N. Engl. J. Med. **245**, 875–878 (1951)
7. R.F. Barth, A.H. Soloway, R.G. Fairchild, R.M. Brugger, Boron neutron capture therapy for cancer: Realities and prospects. Cancer **70**, 2995–3007 (1992). doi:10.1002/1097-0142(19921215)70:12<2995::AID-CNCR2820701243>3.0.CO;2-#
8. T. Kobayashi, K. Kanda, Analytical calculation of boron-10 dosage in cell nucleus of neutron capture therapy. Radiat. Res. **91**, 77–94 (1982). doi:10.2307/3575817
9. D. Gabel, S. Foster, R.G. Fairchild, The Monte Carlo simulation of the biological effect of the 10B(n, α)7Li reaction in cells and tissue and its implication for boron neutron capture therapy. Radiat. Res. **111**, 14–25 (1987). doi:10.2307/3577018
10. J. Capala, J.S. Makar, J.A. Coderre, Accumulation of boron in malignant and normal cells incubated in vitro with boronophenylalanine, mercaptoborane or boric acid. Radiat. Res. **146**, 554–560 (1996). doi:10.2307/3579556
11. P. Panov, Y. Salomon, G.W. Kabalka, P. Bendel, Uptake and washout of borocaptate sodium and borono-phenylalanine in cultured melanoma cells: a multi-nuclear NMR study. Radiat. Res. **154**, 104–112 (2000). doi:10.1667/0033-7587(2000)154[0104:UAWOBS]2.0.CO;2
12. M.F. Hawthorne, M.W. Lee, A critical assessment of boron target compounds for boron neutron capture therapy. J. Neurooncol. **62**, 33–45 (2004)
13. A.H. Soloway, W. Tjarks, B.A. Barnum, F.G. Rong, R.F. Barth, I.M. Codogni, J.G. Wilson, The chemistry of neutron capture therapy. Chem. Rev. **98**, 1515–1562 (1998). doi:10.1021/cr941195u
14. N. Hamada, S.I. Sawada, A. Oshiyama, New one-dimensional conductors: graphitic microtubules. Phys. Rev. Lett. **68**, 1579–1581 (1992). doi:10.1103/PhysRevLett.68.1579
15. M. Terrones, J.M. Romo-Herrera, E. Cruz-Silva, F. López-Urías, E. Muñoz-Sandoval, J.J. Velázquez-Salazar, H. Terrones, Y. Bando, D. Golberg, Pure and doped boron nitride nanotubes. Mater. Today **10**, 30–38 (2007). doi:10.1016/S1369-7021(07)70077-9
16. N.G. Chopra, A. Zettl, Measurement of the elastic modulus of a multi-wall boron nitride nanotube. Solid State Commun. **105**, 297–300 (1998). doi:10.1016/S0038-1098(97)10125-9
17. A.P. Suryavanshi, M.F. Yu, J. Wen, C. Tang, Y. Bando, Elastic modulus and resonance behavior of boron nitride nanotubes. Appl. Phys. Lett. **84**, 2527–2529 (2004). doi:10.1063/1.1691189
18. Y. Chen, J. Zou, S.J. Campbell, G. Le Caer, Boron nitride nanotubes: Pronounced resistance to oxidation. Appl. Phys. Lett. **84**, 2430–2432 (2004). doi:10.1063/1.1667278
19. L. Lacerda, A. Bianco, M. Prato, K. Kostarelos, Carbon nanotubes as nanomedicines: from toxicology to pharmacology. Adv. Drug Deliv. Rev. **58**, 1460–1470 (2006). doi:10.1016/j.addr.2006.09.015
20. D. Golberg, Y. Bando, C. Tang, C. Zhi, Boron nitride nanotubes. Adv. Mater. **19**, 2413–2432 (2007). doi:10.1002/adma.200700179
21. G. Ciofani, V. Raffa, A. Menciassi, P. Dario, Preparation of boron nitride nanotubes aqueous dispersions for biological applications. J. Nanosci. Nanotechnol. (2008). doi:10.1166/jnn.2008.339
22. G. Ciofani, V. Raffa, A. Menciassi, A. Cuschieri, Cytocompatibility, interactions and uptake of polyethyleneimine-coated boron nitride nanotubes by living cells: confirmation of their potential for biomedical applications. Biotechnol. Bioeng. **101**, 850–858 (2008). doi:10.1002/bit.21952
23. S.D. Konda, M. Aref, S. Wang, M. Brechbiel, E.C. Wiener, Specific targeting of folate-dendrimer MRI contrast agents to the high affinity folate receptor expressed in ovarian tumor

xenografts. Magnetic Resonance Materials in Physics. Biol. Med. (Paris) **12**, 104–113 (2001)
24. Y.J. Lu, P.S. Low, Immunotherapy of folate receptor-expressing tumors: Review of recent advances and future prospects. J. Control Release **91**, 17–29 (2003). doi:10.1016/S0168-3659(03)00215-3
25. H. Choi, S.R. Choi, R. Zhou, H.F. Kung, I.W. Chen, Iron oxide nanoparticles as magnetic resonance contrast agent for tumor imaging via folate receptor-targeted delivery. Acad. Radiol. **11**, 996–1004 (2004). doi:10.1016/j.acra.2004.04.018
26. D. Shen, I. Pastan, M.M. Gottesman, Cross-resistance to methotrexate and metals in human cisplatin-resistant cell lines results from a pleiotropic defect in accumulation of these compounds associated with reduced plasma membrane binding proteins. Cancer Res. **58**, 268–275 (1998)
27. Y. Chen, J. Fitz Gerald, J.S. Williams, S. Bulcock, Synthesis of boron nitride nanotubes at low temperatures using reactive ball milling. Chem. Phys. Lett. **299**, 260–264 (1999). doi:10.1016/S0009-2614(98)01252-4
28. J. Yu, Y. Chen, R. Wuhrer, Z. Liu, S.P. Ringer, In situ formation of BN nanotubes during nitriding reactions. Chem. Mater. **17**, 5172–5176 (2005). doi:10.1021/cm050966f
29. J. Pan, S.S. Feng, Targeted delivery of paclitaxel using folate-decorated poly(lactide)evitamin E TPGS nanoparticles. Biomaterials **29**, 2663–2672 (2008). doi:10.1016/j.biomaterials.2008.02.020
30. N.W. Shi Kam, M. Connell, J.A. Wisdom, H. Dai, Carbon nanotubes as multifunctional biological transporters and near-infrared agents for selective cancer cell destruction. Proc. Natl. Acad. Sci. USA **102**, 11600–11605 (2005). doi:10.1073/pnas.0502680102
31. Q. Huang, A.S.D. Sandanayaka, Y. Bando, C.Y. Zhi, R.Z. Ma, G.Z. Shen, D. Golberg, J.C. Zhao, Y. Araki, O. Ito, L. Gao, Donor–acceptor nanoensembles based on boron nitride nanotubes. Adv. Mater. **19**, 934–938 (2007). doi:10.1002/adma.200602058
32. V. Raffa, P. Castrataro, A. Menciassi, P. Dario, Introduction to focused ion beam, in *Applied scanning probe methods*, vol. II, ed. by B. Bushan, H. Fuchs (Springer-Verlag, Heidelberg, 2005), pp. 357–407
33. S.D. Weitman, R.H. Lark, L.R. Coney, D.W. Fort, V. Frasca, V.R. Zurawski, B.A. Kamen, Distribution of the folate receptor GP38 in normal and malignant cell lines and tissues. Cancer Res. **52**, 3396–3401 (1992)
34. J.M. Saul, A. Annapragada, J.V. Natarajan, R.V. Bellamkonda, Controlled targeting of liposomal doxorubicin via the folate receptor in vitro. J. Control Release **92**, 49–67 (2003). doi:10.1016/S0168-3659(03)00295-5
35. K.M. McNeeley, A. Annapragada, R.V. Bellamkonda, Decreased circulation time offsets increased efficacy of PEGylated nanocarriers targeting folate receptors of glioma. Nanotechnology **18**, 385101 (11 pp) (2007)
36. G. Wu, R.F. Barth, W. Yang, R.J. Lee, W. Tjarks, M.V. Backer, J.M. Backer, Boron containing macromolecules and nanovehicles as delivery agents for neutron capture therapy. Anticancer Agents Med. Chem. **6**, 167–184 (2006). doi:10.2174/187152006776119153
37. K.K. Jain, Use of nanoparticles for drug delivery in glioblastoma multiforme. Expert Rev. Neurother. **7**, 363–372 (2007). doi:10.1586/14737175.7.4.363
38. G. Ciofani, V. Raffa, A. Menciassi, A. Cuschieri, Boron nitride nanotubes: an innovative tool for nanomedicine. Nano Today **4**, 8–10 (2009). doi:10.1016/j.nantod.2008.09.001